The added prognostic value of radiological phenotype combined with clinical features and isocitrate dehydrogenase mutation status in anaplastic gliomas

Minsu Lee

Department of Medicine

The Graduate School, Yonsei University

The added prognostic value of radiological phenotype combined with clinical features and isocitrate dehydrogenase mutation status in anaplastic gliomas

Directed by Professor Sung Soo Ahn

The Master's Thesis
submitted to the Department of Medicine
the Graduate School of Yonsei University
in partial fulfillment of the requirements for the degree
of Master of Medical Science

Minsu Lee

December 2017

연세대학교
YONSEI UNIVERSITY

This certifies that the Master's Thesis of
Minsu Lee is approved.

Thesis Supervisor : Sung Soo Ahn

Thesis Committee Member#1 : Jong Hee Chang

Thesis Committee Member#2 : Se Hoon Kim

The Graduate School
Yonsei University

December 2017

ACKNOWLEDGEMENTS

Firstly, I express my gratitude to Professor Sung Soo Ahn, who is my thesis supervisor, for her sincere guidance and advice throughout my thesis. Without her support, this work would not have been completed.

I am also indebted to my committee members, Professor Jong Hee Chang and Professor Se Hoon Kim for their helpful career advice and suggestions in general. In addition, I would like to thank Kyunghwa Han for her help with the statistical support and advices.

Finally, I appreciate my family for everlasting trust and support, which deserve my sincere gratitude.

<TABLE OF CONTENTS>

LIST OF FIGURES

LIST OF TABLES

ABSTRACT

The added prognostic value of radiological phenotype combined with clinical features and isocitrate dehydrogenase mutation status in anaplastic gliomas

Minsu Lee

Department of Medicine
The Graduate School, Yonsei University

(Directed by Professor Sung Soo Ahn)

Purpose: Previous studies have demonstrated the potential of magnetic resonance image (MRI) features in predicting survival in anaplastic gliomas. The aim of this study was to investigate whether identifying radiological phenotype improved predictability when added to the prognostic model based on isocitrate dehydrogenase (IDH) mutation status.

Methods: Preoperative MR images of 86 patients with anaplastic gliomas (WHO grade III) and known IDH mutation status were analyzed according to the Visually Accessible Rembrandt Images (VASARI) features set. Radiological risk scores were calculated for overall survival (OS) and progression-free survival (PFS) using the least absolute shrinkage and selection operator Cox regression model. Multivariate Cox analysis included age, preoperative performance status, extent of resection, IDH mutation status, and radiological risk score. The added predictive value of radiological risk score was calculated by comparing C-indices between Cox models with and without radiological risk score.

Results: Eight VASARI features contributed to radiological risk score for OS, and six contributed to PFS. For both OS and PFS, tumor

multifocality or multicentricity was the most influential feature, followed by restricted diffusion. In multivariate Cox analyses, age, IDH mutation status, and radiological risk score were independent predictors of survival. Multivariate Cox models with radiological risk score demonstrated significantly higher survival prediction than models without (C-index: 0.893 vs. 0.831 for OS; 0.823 vs. 0.752 for PFS).

Conclusions: Radiological risk scores derived from MRI features were independent predictors of survival in patients with anaplastic gliomas. The addition of radiological risk score to the IDH-based prognostic model significantly improved predictive performance.

Key words : anaplastic glioma; magnetic resonance imaging; IDH mutation; image biomarker; VASARI

The added prognostic value of radiological phenotype combined with clinical features and isocitrate dehydrogenase mutation status in anaplastic gliomas

Minsu Lee

Department of Medicine
The Graduate School, Yonsei University

(Directed by Professor Sung Soo Ahn)

I. INTRODUCTION

Anaplastic gliomas account for approximately 5% of all primary brain tumors and are generally associated with poor prognosis. Tumor recurrence or progression to grade IV glioblastoma is frequently observed within several years of diagnosis.[1] Anaplastic gliomas are generally treated with the maximum-safe-resection approach to surgery plus radiotherapy. Occasionally, adjuvant systemic chemotherapy is added according to the tumor subtype.[2] Patient age, performance status, and extent of surgical resection have been proposed as clinical prognostic factors.[3,4]

The median survival rate of patients with anaplastic glioma is between 15 and 42 months, which is highly variable even among those with the same pathological diagnosis.[4] Since the late 2000s, several studies have revealed that the outcome of anaplastic glioma is more closely related to molecular biomarkers than pathological diagnosis.[3,5-7] Among these, isocitrate dehydrogenase (IDH) mutation status is known to have the most significant prognostic relevance. Positive IDH mutation within glioma tissue is an indicator of favorable prognosis in diffuse lower-grade glioma, while tumors with wild-type IDH exhibit a poor clinical outcome comparable with glioblastoma.[8] According to these results, the latest update of the WHO classification adopted molecular

parameters and generated an integrated diagnosis combining phenotypic and genotypic classifications.[9]

Anaplastic gliomas also exhibit morphological heterogeneity on imaging. Therefore, reliable imaging biomarkers are necessary for noninvasive risk stratification and personalized treatment planning. To date, a few MRI features have been proposed to have predictive value for survival and tumor genotype. Pope et al[10] analyzed the association between 15 MRI variables of high-grade glioma with survival. The results showed that the presence of noncontrast-enhancing tumor (nCET), absence of necrosis, and absence of multifocal or satellite lesions were associated with improved survival. Wang et al[11] evaluated patterns of tumor contrast enhancement and revealed its predictive value for patient survival.

Because the incidence of anaplastic glioma is significantly lower than glioblastoma, more reproducible and validated image assessment is required for data accumulation and comparison. In glioblastoma, several studies have adopted a united terminology provided by the Visually Accessible Rembrandt Images research project (VASARI lexicon), which provides standardized grading of visual MRI findings in glioma.[12-15] The VASARI lexicon is currently the most sophisticated descriptive system, consisting of 26 qualitative features from standard contrast-enhanced MRI. The VASARI lexicon has also been introduced in lower-grade gliomas. In a recent study, Zhou et al[16] analyzed MRI features of diffuse lower-grade gliomas (WHO II or III) according to VASARI lexicon, demonstrating associations with survival and molecular profile.

The purpose of the present study was to investigate the prognostic value of MRI features assessed using the VASARI lexicon in anaplastic glioma combined with IDH mutation status and clinical risk factors.

II. MATERIALS AND METHODS

1. Patients

This study was approved by our institutional review board; however, given its

retrospective nature, requirement for informed consent was waived. We reviewed institutional electronic medical records of 145 consecutive patients with pathologically confirmed anaplastic glioma (WHO grade III) between January 2007 and February 2016 and available preoperative MR images. Among these, 59 patients were excluded for the following reasons: unknown IDH mutation status (n=33); previous diagnosis of any brain tumor (n=20); lack of diffusion-weighted imaging (DWI) data or diffusion tensor imaging (DTI) data in the MRI sequence (n=3); and age younger than 18 years (n=3). In total, 86 consecutive patients (mean age 44.5 years [range, 20-78 years]), including 50 men (mean age 44.3 years [range, 20-76 years]) and 36 women (mean age 44.9 years [range, 21-78 years]) were identified. The patient selection process is presented in Figure 1 along with IDH mutation status. Demographic variables and performance scores (Karnofsky Performance Score [KPS]) were evaluated by electronic medical record review. Eighty-four patients received postoperative adjuvant therapy; 56 (65.1%) underwent radiation therapy; 28 (32.6%) underwent concurrent chemoradiation with either a combination of procarbazine, lomustine and vincristine (n=15), or temozolomide (n=13); and 2 (2.3%) patients refused additional treatment. The extent of tumor resection was assessed by visually comparing the preoperative and postoperative volume of the lesion on contrast-enhanced T1-weighted imaging as well as the surgeon's intraoperative impressions: total, subtotal (<100% and ≥75% removal of radiological tumor volume), partial resection (<75% removal), and biopsy only.

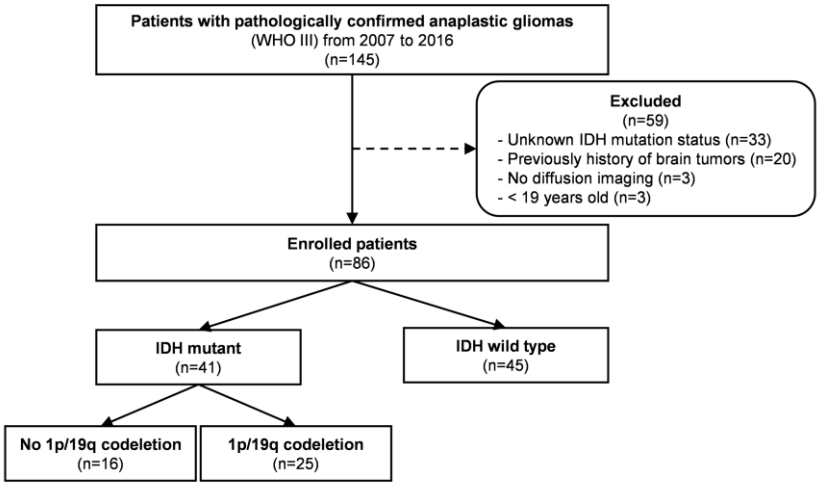

Figure 1. Flow diagram of patient selection.

2. MR image acquisition

Preoperative MRI was performed using a 3.0 T MRI device (Achieva, Philips Medical Systems, Best, the Netherlands) equipped with an eight-channel sensitivity-encoding head coil. The preoperative MRI protocol included T1-weighted (repetition time [TR]/echo time [TE], 1800-2000/10-15 ms; field of view, 240 mm; section thickness, 5 mm; matrix, 256 × 256), T2-weighted (TR/TE 2800-3000/80-100 ms; field of view, 240 mm; section thickness, 5 mm; matrix, 256 × 256), and fluid-attenuated inversion recovery (FLAIR) (TR/TE 9000-10000/110-125 ms; field of view, 240 mm; section thickness, 5 mm; matrix, 256 × 256) images. Three-dimensional contrast-enhanced T1-weighted images (TR/TE 6.3-8.3/3.1-4 ms; field of view, 240 mm; section thickness, 1 mm; matrix, 192 × 192) were acquired after administering 0.1 mL/kg gadolinium-based contrast material (Gadovist, Bayer, Toronto, Ontario, Canada). Diffusion tensor imaging (DTI) was obtained using b values of 600 sec/mm2 and 0 sec/mm2, 32 directions, and the following parameters: TR/TE 8413.4/77 ms; field of view, 220 mm; section thickness, 2 mm; and matrix, 112 × 112.

Postoperative MR images were acquired 48 h to 72 h after surgery in all patients.

3. Image analysis

Two board-certified neuroradiologists (S.S.A. [10 years' experience], S.H.B [5 years' experience]) blinded to the patients' clinical information independently reviewed the MR images of all patients according to the VASARI features set. The exact description of all the features can be found at the National Cancer Institute's Cancer Imaging Archive <https://wiki.cancerimagingarchive.net/display/Public/VASARI+Research+Project>. The following MRI features of VASARI were used: major and minor axis lengths; tumor location; side of tumor epicenter; eloquent brain; enhancement quality; proportion of contrast-enhancing tumor (CET); proportion of nCET; proportion of edema; proportion of necrosis; cysts; multifocal or multicentric; T1/FLAIR ratio; definition of nonenhancing margin; hemorrhage; diffusion characteristics; pial invasion; ependymal extension; cortical involvement; deep white matter invasion; nCET crossing midline; CET crossing midline; satellites; and calvarial remodeling. Briefly, tumor location with regard to involvement with the eloquent cortex was defined as the presence of tumor involvement with the eloquent cortex, or immediate subcortical white matter of the eloquent cortex of speech motor, speech receptive, motor, and vision. Edema had to be greater in signal than the nCET and lower in signal than cerebrospinal fluid on T2-weighted images. nCET was defined by regions of T2 hyperintensity (less than the intensity of the cerebrospinal fluid) that were associated with mass effect and architectural distortion, including blurring of the gray-white matter interface. Multifocality was defined as at least one region of tumor not contiguous with the dominant lesion, resulting from dissemination along an established route, including white matter tracts, grey matter, the ventricular systems, or meninges. Multicentricity referred to widely separated lesions without explainable tract. A satellite lesion was defined as an area of enhancement within the region of signal abnormality surrounding the dominant lesion but not contiguous with any part of the dominant tumor mass. Deep white

matter involvement was defined when a CET or nCET extended into the internal capsule, corpus callosum, or brain stem. Ependymal involvement was defined if the contrast-enhancing or nonenhancing lesion contacted the lining of the ventricles. Results with discrepancies were resolved by consensus agreement of the reviewers.

4. Pathological evaluation and molecular subtyping

All surgical specimens were histopathologically diagnosed according to the 2016 WHO classification. For molecular subtyping, IDH1/2 mutation status, and chromosomal status of 1p and 19q, were assessed. Both peptide nucleic acid-mediated clamping polymerase chain reaction and immunohistochemical analysis were performed to detect the IDH1 R132H mutation.[17] Monoclonal antibody H09 was used for immunohistochemical analysis. The degree of IDH1-R132H staining was determined in cases exhibiting any cell rated to be positive; cases without IDH1-R132H staining were rated as negative.[18] If immunohistochemical staining demonstrated negative results in IDH1 mutation analysis, IDH1/2 status was confirmed by peptide nucleic acid-mediated clamping polymerase chain reaction. Fluorescence in situ hybridization analysis was used for investigation of 1p/19q codeletion.[19]

5. Definition of survival

Progression-free survival (PFS) and overall survival (OS) were used as parameters of clinical outcome. OS was defined as the number of days between the date of the initial diagnostic surgery and that of death or the last follow-up. PFS was defined as the number of days between the initial diagnostic surgery and that of tumor progression, death, or the date of the last follow-up if the patient did not experience disease progression or death. Tumor progression was defined according to response assessment in the neuro-oncology (RANO) criteria.[20] A neuroradiologist (S.S.A) determined the date of tumor progression.

6. Statistical analysis

The inter-rater agreement for imaging features was assessed using the kappa (κ) consistency test. Categorical variables with > 2 categories were dichotomized using Kaplan-Meier analysis and log-rank test at the point where the prognosis was best distinguished. Because of the relatively large number of statistically significant imaging variables compared with the number of events, the least absolute shrinkage and selection operator (LASSO) Cox regression model was used to select features with more significance to minimize the potential risk for overfitting. The performance of the LASSO model was tested by 5-fold cross-validation. The lambda value at the point of the lowest partial likelihood was selected and significant variables were extracted. A radiological risk score (RRS) was calculated for each patient through a linear combination of selected features weighted according to their regression coefficients. The optimal cutoff value of the RRS was defined by log-rank test, according to a method previously published by Contal and O'Quigley.[21] Multivariate Cox regression was used to generate a prognostic model including age, KPS, extent of resection, IDH mutation, and RRS. The added value of RRS was calculated by comparing C-indices between multivariate Cox models with and without RRS. The difference in C-indices was validated using bootstrap analysis with 1,000 resampling estimates. Statistical analysis was performed using R software, version 3.3.2 (www.R-project.org); $P < 0.05$ was considered to be statistically significant.

III. RESULTS

Characteristics of the 86 enrolled patients are summarized in Table 1. According to the molecular categories, 45 patients were anaplastic astrocytoma, IDH-wild type; 25 were anaplastic oligodendroglioma, IDH mutant with 1p/19q codeletion; and 16 were anaplastic astrocytoma, IDH mutant without 1p/19q codeletion. The median OS was 664 days and median PFS was 568.5 days.

Interobserver agreements for the VASARI features were evaluated, and were good to excellent. The imaging features with the highest interobserver agreement were

tumor location, side of tumor epicenter, and calvarial remodeling (κ = 1.0); the lowest interobserver agreement was found in the proportion of edema (κ = 0.662).

Table 1. Patient Characteristics

Variables	No. of patients (n=86)
Age (years)*	44.5 ± 14.4
Sex	
Male	50 (58.1)
Female	36 (41.9)
Karnofsky performance status*	78.6 ± 9.7
Median OS (days)	664
No. deaths	27 (31.4)
Median PFS (days)	568.5
No. tumor progression	40 (46.5)
IDH mutation status	
Mutant	41 (47.7)
1p/19q codeletion	25
No 1p/19q codeletion	16
Wild type	45 (52.3)
Extent of Resection	
Total	65 (75.6)
Subtotal	8 (9.3)
Partial	4 (4.6)
Biopsy	9 (10.5)

* Data are mean ± SD. Unless otherwise indicated, data are presented as numbers of patients (%).

1. Radiologic risk score (RRS) for overall survival (OS)

In the LASSO Cox regression model including VASARI features, the following 8 features revealed significant relationships with OS: nonlobar tumor location; proportion of CET > 33%; proportion of edema > 33%; multifocal or multicentric distribution (i.e., nonfocal distribution); restricted diffusion; pial invasion; ependymal extension; and cortical involvement. The following RRS

was derived from the LASSO model, weighted with the regression coefficient. The regression coefficient of each feature is shown in Figure 2A:

RRS for OS (RRS_OS) = Nonlobar location*0.221 + CET > 33%*0.380 + edema > 33%*0.112 + nonfocal distribution*1.673 + restricted diffusion*0.725 - pial invasion*0.019 + ependymal extension*0.386 – cortical involvement*0.415

The optimal cutoff value generated by log-rank test to stratify prognosis was 0.3. Based on this, patients were classified into a high-risk group (RRS_OS ≥ 0.3) or low-risk group (RRS_OS < 0.3). The low-risk group had longer OS than the high-risk group according to log-rank test (P<0.001) (Figure 3B). The median OS period was 963 days for the low-risk group and 484 days for the high-risk group.

2. Radiologic risk score (RRS) for progression-free survival (PFS)

Six imaging features of VASARI demonstrated significant relationships with PFS: nonlobar tumor location; proportion of CET > 33%; multifocal or multicentric distribution (nonfocal distribution); poor definition of nCET margin; restricted diffusion; and ependymal extension. The RRS for PFS was calculated according to the following equation; the regression coefficient of each feature is shown in Figure 2B:

RRS for PFS (RRS_PFS) = Nonlobar location*0.144 + CET > 33*0.055 + nonfocal distribution*1.375 + poor nCET margin *0.067 + restricted diffusion*0.771 + ependymal extension*0.055

The optimal cutoff value generated by log-rank test was 0.18. Accordingly, patients were divided into a high-risk group (RRS_PFS ≥ 0.18) or low-risk group (RRS_PFS < 0.18). The low-risk group had a longer PFS than the high-risk group according to log-rank test (P<0.001) (Figure 3D). The median PFS period was 931 days for the low-risk group and 382 days for the high-risk

group.

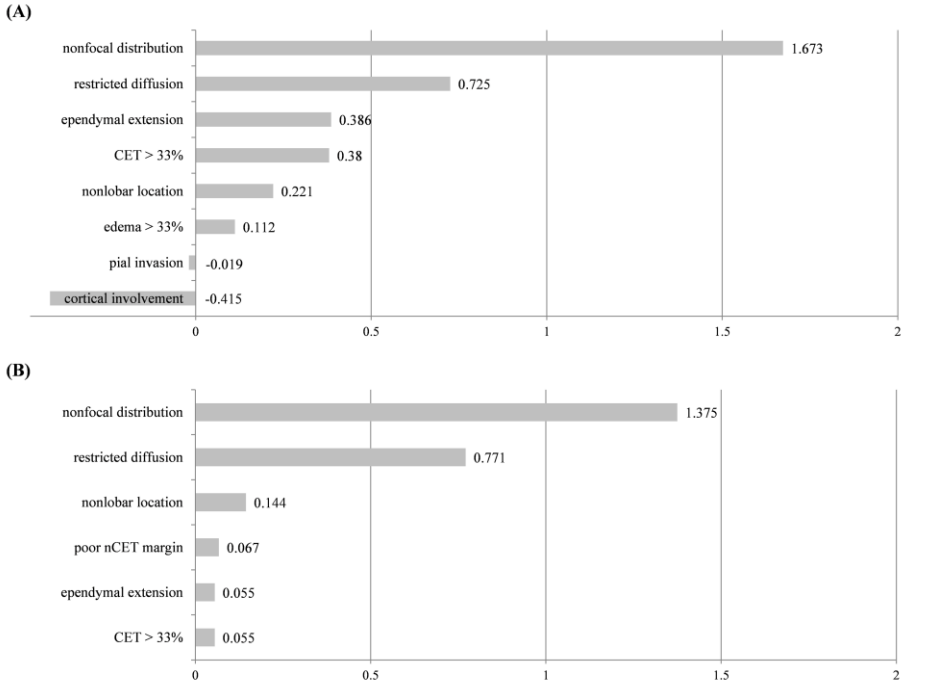

Figure 2. Histograms demonstrating the contribution of each imaging parameter in constructing radiological risk scores (RRSs) for overall survival (OS) (A) and progression-free survival (PFS) (B). Values are the coefficients obtained from least absolute shrinkage and selection operator (LASSO) Cox analysis.

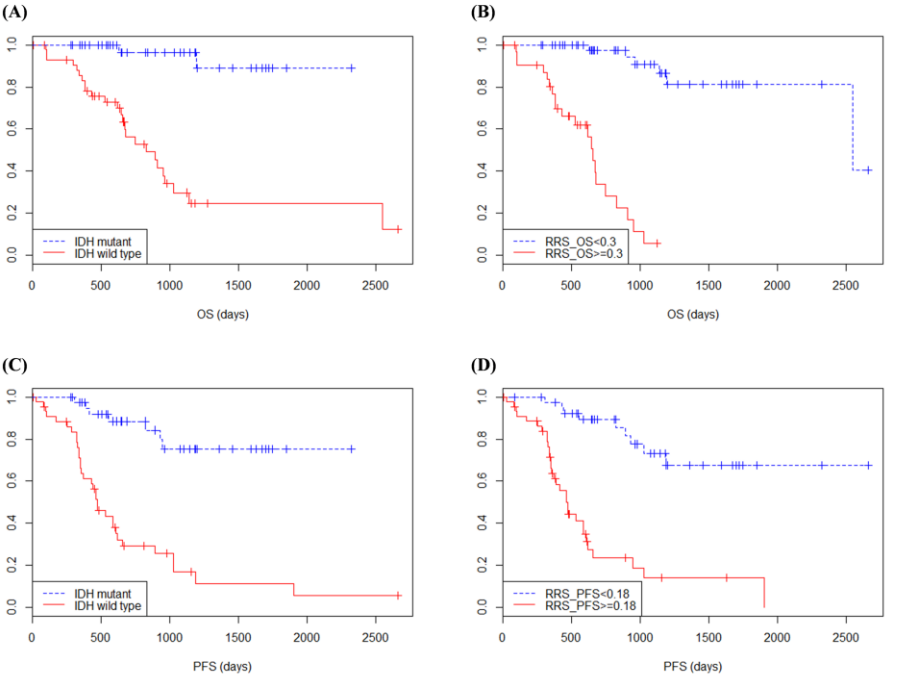

Figure 3. Kaplan-Meier curves of isocitrate dehydrogenase (IDH) mutational status and radiological risk scores (RRSs) for overall survival (OS) (A, B) and progression-free survival (PFS) (C, D). RRSs were significant prognostic factors for OS and PFS as well as IDH mutation status.

3. Added value of RRS in predicting OS

Multivariate Cox models with and without RRS_OS are summarized in Table 2. The predictive performance of the multivariate Cox model was significantly improved by adding RRS_OS to the clinical features and IDH1/2 mutation status. In a model with age, KPS, extent of resection and IDH1/2 mutation, the C-index was 0.831 (95% CI 0.752–0.902). When RRS_OS was added to this model, the C-index was elevated to 0.893 (95% CI 0.830–0.957). In bootstrap testing, the increase in C-index was statistically significant (change in C-index: 0.062 [95% CI 0.016–0.143). Age (≥ 65 years) (P≤0.001), RRS_OS (P<0.001), and IDH1/2 mutation (P=0.049) were significantly associated with OS.

Table 2. Comparison of Multivariate Cox Models with and without Radiological Risk Score for OS (RRS_OS)

Variables	Model 1			Model 2		
	HR	95% CI	P value	HR	95% CI	P value
Age ≥65	3.614	1.085-12.034	0.036	15.523	3.023-50.291	<.001
KPS ≥80	1.303	0.497-3.416	0.590	0.725	0.306-1.936	0.582
Total tumor resection	0.490	0.210-1.149	0.101	1.064	0.422-4.550	0.915
IDH mutation	0.074	0.017-0.331	<.001	0.189	0.030-0.742	0.049
RRS_OS				5.887	2.473-7.806	<.001
C-index	0.831 (95% CI, 0.752-0.902)			0.893 (95% CI, 0.830-0.957)		
C-index difference	0.062 (95% CI, 0.016-0.143)					

Model 1 = age + KPS + extent of resection + IDH mutation status
Model 2 = age + KPS + extent of resection + IDH mutation status + radiologic risk score for OS
KPS = Karnofsky performance status, IDH = Isocitrate dehydrogenase, HR = hazard ratio, CI = confidence interval.

4. Added value of RRS in predicting PFS

Multivariate Cox models with and without RRS_PFS are summarized in Table 3. With RRS_PFS, the predictability of the multivariate Cox model was significantly increased. In a model with age, KPS, extent of resection, and IDH1 mutation, the C-index was 0.752 (95% CI 0.684–0.841). When RRS_PFS was added to this model, the C-index was elevated to 0.823 (95% CI 0.744–0.892). In bootstrap testing, the increase in C-index was statistically significant (change in C-index: 0.071 [95% CI 0.010–0.116]). RRS_PFS (P<0.001), age (≥ 65 years) (P=0.005), and IDH1/2 mutation (P=0.018) were significantly associated with PFS.

Table 3. Comparison of Multivariate Cox Models with and without Radiological Risk Score for PFS (RRS_PFS)

Variables	Model 1			Model 2		
	HR	**95% CI**	**P value**	**HR**	**95% CI**	**P value**
Age ≥65	2.468	0.929-6.557	0.070	4.314	1.540-12.087	0.005
KPS ≥80	1.231	0.565-2.684	0.601	0.706	0.298-1.674	0.429
Total tumor resection	0.482	0.229-1.010	0.053	1.348	0.523-3.474	0.536
IDH mutation	0.202	0.085-0.481	<.001	0.330	0.131-0.828	0.018
RRS_PFS				3.181	1.882-5.377	<.001
C-index	0.752 (95% CI,0.684-0.841)			0.823 (95% CI, 0.744-0.892)		
C-index difference	0.071 (95% CI, 0.010-0.116)					

Model 1 = age + KPS + extent of resection + IDH mutation status
Model 2 = age + KPS + extent of resection + IDH mutation status + radiologic risk score for PFS
KPS = Karnofsky performance status, IDH = Isocitrate dehydrogenase, HR = hazard ratio, CI = confidence interval.

IV. DISCUSSION

In this study, we examined the prognostic value of preoperative MRI features in patients with anaplastic glioma. RRS derived from MRI features was an independent predictor of OS and PFS, which may help predict prognosis in patients with anaplastic glioma preoperatively. In addition, the predictive performance of the survival model was significantly improved by adding RRS to a model consisting only of clinical features and IDH mutation status.

Among the VASARI features, several imaging features were significantly associated with survival. For both OS and PFS, nonfocal distribution (i.e.,

multifocality or multicentricity) had the greatest effect on RRS, followed by restricted diffusion within the tumor. Considering that the obtained cutoff values were 0.3 for RRS_OS and 0.18 for RRS_PFS, patients with any of the above 2 features were in the high risk group, virtually regardless of other findings. In addition, ependymal extension, proportion of CET >33%, nonlobar location, and proportion of edema >33% were factors that increased RRS_OS; cortical involvement and pial invasion lowered RRS_OS. Nonlobar location, poor definition of nCET margin, ependymal extension, and proportion of CET >33% increased RRS_PFS.

According to our results, multifocality or multicentricity was an imaging feature that significantly impacted prognosis. However, their prognostic significance is not clearly understood in anaplastic gliomas. Pope et al[10] reported that multifocality was a statistically significant predictor of poor survival only in a univariate analysis of their limited pool of patients with anaplastic glioma. In glioblastoma, some authors have reported the prognostic value of tumor multifocality or multicentricity.[22,23] Here, we report that tumor with multifocal or multicentric distribution could also be a key imaging feature suggesting high risk in anaplastic gliomas.

Diffusion restriction was the second most influential factor in RRS. DWI is a technique that visualizes the microscopic motion of free water molecules. Water diffusibility is measured by the apparent diffusion coefficient (ADC) value, which is a quantitative parameter calculated from DWI. As cells within a tissue increase in size or number, the motion of free water molecules in the extracellular space is disturbed by cell membranes, resulting in a decrease in ADC value. According to a previous study by Sugahara et al,[24] ADC values were found to be negatively correlated with the cellularity and grade of glioma. In addition, there are several reports that ADC value is correlated with prognosis in malignant astrocytoma, including anaplastic astrocytomas and glioblastoma.[25,26] Our results also demonstrated the prognostic significance of DWI in patients with anaplastic gliomas.

The importance of the subventricular zone (SVZ), which is rich in neural stem

cells, has been emphasized since the cancer stem cell theory was proposed in glioma.[27] Tumors in contact with the SVZ tend to be highly invasive, multifocal, and exhibit poor OS in glioblastoma.[28,29] In addition, a recent study reported an association with SVZ involvement and poor prognostic outcome in anaplastic glioma.[30] In our study, the presence of ependymal tumor extension was a negative predictor for both OS and PFS. This is generally consistent with previous reports, although ependymal extension in VASARI lexicon is not exactly the same with SVZ involvement.

IDH1 and IDH2 are enzymes that catalyze the oxidative decarboxylation of isocitrate, producing alpha-ketoglutarate. IDH mutation status is a key genotypic feature in the classification of diffuse astrocytic and oligodendroglial tumors. It was also a significant discriminator of prognosis in our study population. It showed independent statistical importance in a multivariate Cox model including age, KPS, and extent of resection.

RRS, a compressed representation of MR features, significantly improved the predictive performance of the survival model including clinical features and IDH mutation status. It was also an excellent discriminator of high-risk patients. To date, studies investigating imaging risk factors have focused on evaluating prognostic performance for each image finding. A recent study examining radiomics features of early-stage non-small cell lung cancer reported that integrated radiological score could be an independent biomarker, even in cases in which individual features failed to demonstrate statistical significance with prognosis.[31] We focused on this point and attempted to discover meaningful radiological features broadly by using LASSO. As a result, a relatively large number of imaging features—eight for OS and six for PFS—were extracted compared with previous VASARI-based imaging studies.[15,16] We revealed the prognostic value of an integrated RRS in patients with anaplastic glioma. Adding an RRS to a survival model including IDH mutation status enables a more detailed classification of anaplastic glioma, which is currently understood as a group of diseases with heterogeneous prognosis.

There were a few limitations to our study, the first of which was its retrospective

design and relatively small sample size. Although a prospective design would be preferred, it was difficult due to the low incidence of anaplastic glioma and variable prognoses. The disadvantages of small sample size were complemented by statistical techniques such as cross-validation and bootstrapping. Second, due to the retrospective design, the postoperative treatment regimens were not uniform. In particular, some of the patients without the 1p/19q codeletion were administered temozolomide concurrently with radiotherapy. Although the number is small, we cannot rule out the possibility that these patients may have affected the outcome. Finally, only a visual, qualitative assessment of the DWI and ADC map was performed. Further study to evaluate prognostic values of ADC using quantitative analysis, such as histogram, is warranted in anaplastic gliomas.

V. CONCLUSION

In conclusion, RRS derived from MRI features was an independent prognostic factor in patients with anaplastic glioma. The addition of RRS to clinical features and IDH mutation status significantly improved the predictability of survival.

REFERENCES

1. DeAngelis LM. Anaplastic glioma: how to prognosticate outcome and choose a treatment strategy. [corrected]. J Clin Oncol 2009;27:5861-2.
2. Rhun EL, Taillibert S, Chamberlain MC. The future of high-grade glioma: Where we are and where are we going. Surgical Neurology International 2015;6:S9-S44.
3. Wick W, Hartmann C, Engel C, Stoffels M, Felsberg J, Stockhammer F, et al. NOA-04 randomized phase III trial of sequential radiochemotherapy of anaplastic glioma with procarbazine, lomustine, and vincristine or temozolomide. J Clin Oncol 2009;27:5874-80.
4. Nuno M, Birch K, Mukherjee D, Sarmiento JM, Black KL, Patil CG. Survival and prognostic factors of anaplastic gliomas. Neurosurgery 2013;73:458-65; quiz 65.
5. Yan H, Parsons DW, Jin G, McLendon R, Rasheed BA, Yuan W, et al. IDH1 and IDH2 mutations in gliomas. N Engl J Med 2009;360:765-73.
6. Cairncross G, Wang M, Shaw E, Jenkins R, Brachman D, Buckner J, et al. Phase III trial of chemoradiotherapy for anaplastic oligodendroglioma: long-term results of RTOG 9402. J Clin Oncol 2013;31:337-43.
7. van den Bent MJ, Brandes AA, Taphoorn MJ, Kros JM, Kouwenhoven MC, Delattre JY, et al. Adjuvant procarbazine, lomustine, and vincristine chemotherapy in newly diagnosed anaplastic oligodendroglioma: long-term follow-up of EORTC brain tumor group study 26951. J Clin Oncol 2013;31:344-50.
8. Cancer Genome Atlas Research N, Brat DJ, Verhaak RG, Aldape KD, Yung WK, Salama SR, et al. Comprehensive, Integrative Genomic Analysis of Diffuse Lower-Grade Gliomas. N Engl J Med 2015;372:2481-98.
9. Louis DN, Perry A, Reifenberger G, von Deimling A, Figarella-Branger D, Cavenee WK, et al. The 2016 World Health Organization Classification of Tumors of the Central Nervous System: a summary. Acta Neuropathol 2016;131:803-20.
10. Pope WB, Sayre J, Perlina A, Villablanca JP, Mischel PS, Cloughesy TF. MR imaging correlates of survival in patients with high-grade gliomas. AJNR Am J Neuroradiol 2005;26:2466-74.
11. Wang Y, Wang K, Wang J, Li S, Ma J, Dai J, et al. Identifying the association between contrast enhancement pattern, surgical resection, and prognosis in anaplastic glioma patients. Neuroradiology 2016;58:367-74.
12. Gutman DA, Cooper LA, Hwang SN, Holder CA, Gao J, Aurora TD, et al. MR imaging predictors of molecular profile and survival: multi-institutional study of the TCGA glioblastoma data set. Radiology 2013;267:560-9.

13. Mazurowski MA, Desjardins A, Malof JM. Imaging descriptors improve the predictive power of survival models for glioblastoma patients. Neuro Oncol 2013;15:1389-94.
14. Jain R, Poisson LM, Gutman D, Scarpace L, Hwang SN, Holder CA, et al. Outcome prediction in patients with glioblastoma by using imaging, clinical, and genomic biomarkers: focus on the nonenhancing component of the tumor. Radiology 2014;272:484-93.
15. Wangaryattawanich P, Hatami M, Wang J, Thomas G, Flanders A, Kirby J, et al. Multicenter imaging outcomes study of The Cancer Genome Atlas glioblastoma patient cohort: imaging predictors of overall and progression-free survival. Neuro Oncol 2015;17:1525-37.
16. Zhou H, Vallieres M, Bai HX, Su C, Tang H, Oldridge D, et al. MRI features predict survival and molecular markers in diffuse lower-grade gliomas. Neuro Oncol 2017.
17. Yan H, Parsons DW, Jin G, McLendon R, Rasheed BA, Yuan W, et al. IDH1 and IDH2 mutations in gliomas. New England Journal of Medicine 2009;360:765-73.
18. Takano S, Tian W, Matsuda M, Yamamoto T, Ishikawa E, Kaneko MK, et al. Detection of IDH1 mutation in human gliomas: comparison of immunohistochemistry and sequencing. Brain tumor pathology 2011;28:115-23.
19. Riemenschneider MJ, Jeuken JW, Wesseling P, Reifenberger G. Molecular diagnostics of gliomas: state of the art. Acta neuropathologica 2010;120:567-84.
20. Wen PY, Macdonald DR, Reardon DA, Cloughesy TF, Sorensen AG, Galanis E, et al. Updated response assessment criteria for high-grade gliomas: response assessment in neuro-oncology working group. J Clin Oncol 2010;28:1963-72.
21. Contal C, O'Quigley J. An application of changepoint methods in studying the effect of age on survival in breast cancer. Computational Statistics & Data Analysis 1999;30:253-70.
22. Patil CG, Yi A, Elramsisy A, Hu J, Mukherjee D, Irvin DK, et al. Prognosis of patients with multifocal glioblastoma: a case-control study. J Neurosurg 2012;117:705-11.
23. Hassaneen W, Levine NB, Suki D, Salaskar AL, de Moura Lima A, McCutcheon IE, et al. Multiple craniotomies in the management of multifocal and multicentric glioblastoma. Clinical article. J Neurosurg 2011;114:576-84.
24. Sugahara T, Korogi Y, Kochi M, Ikushima I, Shigematu Y, Hirai T, et al. Usefulness of diffusion-weighted MRI with echo-planar technique in the evaluation of cellularity in gliomas. J Magn Reson Imaging 1999;9:53-60.
25. Higano S, Yun X, Kumabe T, Watanabe M, Mugikura S, Umetsu A, et

al. Malignant astrocytic tumors: clinical importance of apparent diffusion coefficient in prediction of grade and prognosis. Radiology 2006;241:839-46.

26. Murakami R, Sugahara T, Nakamura H, Hirai T, Kitajima M, Hayashida Y, et al. Malignant Supratentorial Astrocytoma Treated with Postoperative Radiation Therapy: Prognostic Value of Pretreatment Quantitative Diffusion-weighted MR Imaging. Radiology 2007;243:493-9.
27. Sanai N, Alvarez-Buylla A, Berger MS. Neural stem cells and the origin of gliomas. N Engl J Med 2005;353:811-22.
28. Young GS, Macklin EA, Setayesh K, Lawson JD, Wen PY, Norden AD, et al. Longitudinal MRI evidence for decreased survival among periventricular glioblastoma. Journal of Neuro-Oncology 2011;104:261-9.
29. Jafri NF, Clarke JL, Weinberg V, Barani IJ, Cha S. Relationship of glioblastoma multiforme to the subventricular zone is associated with survival. Neuro Oncol 2013;15:91-6.
30. Liu S, Wang Y, Fan X, Ma J, Qiu X, Jiang T. Association of MRI-classified subventricular regions with survival outcomes in patients with anaplastic glioma. Clin Radiol 2017;72:426 e1- e6.
31. Huang Y, Liu Z, He L, Chen X, Pan D, Ma Z, et al. Radiomics Signature: A Potential Biomarker for the Prediction of Disease-Free Survival in Early-Stage (I or II) Non-Small Cell Lung Cancer. Radiology 2016;281:947-57.

ABSTRACT(IN KOREAN)

역형성 신경교종 환자에서 임상적 위험인자 및 IDH 변이여부에 더하여 영상의학적 소견이 갖는 예후인자로서의 가치 평가

<지도교수 안 성 수>

연세대학교 대학원 의학과

이 민 수

연구 배경 : 역형성 신경 교종의 자기공명영상 (MRI) 소견이 예후를 예측하는 데 이용될 수 있다는 점이 이전 연구들에서 보고되어 있다. 이 연구에서는 이소시트르산탈수소효소 (IDH) 돌연변이 상태에 기초한 기존의 예후 모델에 영상의학적 표현형을 더했을 때 예후 예측력이 향상되는지 여부에 대해 조사하였다.

대상과 방법 : 후향적 연구로서 IDH 돌연변이 상태가 알려진 역형성 신경 교종 환자 86 명을 대상으로 하였다. 이들의 수술 전 MR 영상을 VASARI 에서 제공하는 영상 분석 틀에 따라 분석 하였다. 다양한 영상 변수들 중 의미있는 변수만을 추리기 위하여 LASSO 콕스 회기분석을 이용하였다. 이렇게 얻어진 영상 변수들을 조합하여 영상위험점수 (RRS) 를 전체생존 (OS) 및 무진행생존 (PFS)에 대하여 각각 계산하였다. 나이, 수술 전의 Karnofsky 수행능력 점수, 절제 범위, IDH 돌연변이 상태를 포함한 다변량 콕스 회기분석 모델에 영상위험점수가 추가되었을 때의 C-index의 증가량을 계산하였다

결과 : 전체생존의 경우 8개의 MRI 영상소견이 영상위험점수를 구성하였으며 무진행생존의 경우 6개의 MRI 소견이 영상위험점수를 구성하였다. 전체생존 및 무진행생존 모두에서 종양의 다원성 또는 다중심성이 가장 연관성이 깊은 특징이었고

확산제한이 있는 경우가 그 뒤를 따랐다. 다변량 콕스 회기분석에서 IDH 돌연변이 여부와 영상위험점수는 독립적인 예후 인자였다. 방사선 위험 점수가 포함된 다변량 콕스 모델은 그렇지 않은 모델에 비해 유의하게 높은 생존 예측을 보였다
결론 : 역형성 신경 교종 환자에서 MRI 영상소견으로 계산한 영상위험점수는 독립적인 예후 인자였다. IDH 기반의 예후 모델에 영상위험점수를 추가하였을 때 보다 우수한 예후 예측 능력을 보여주었다.

핵심되는 말 : 역형성 신경교종, 자기공명영상, 이소시트르산탈수소효소 돌연변이, 영상예후인자, VASARI